NBS TECHNICAL NOTE 660

U.S. DEPARTMENT OF COMMERCE / National Bureau of Standards

Molecular Beam Tube Frequency Biases Due To Distributed Cavity Phase Variations

NATIONAL BUREAU OF STANDARDS

The National Bureau of Standards[1] was established by an act of Congress March 3, 1901. The Bureau's overall goal is to strengthen and advance the Nation's science and technology and facilitate their effective application for public benefit. To this end, the Bureau conducts research and provides: (1) a basis for the Nation's physical measurement system, (2) scientific and technological services for industry and government, (3) a technical basis for equity in trade, and (4) technical services to promote public safety. The Bureau consists of the Institute for Basic Standards, the Institute for Materials Research, the Institute for Applied Technology, the Institute for Computer Sciences and Technology, and the Office for Information Programs.

THE INSTITUTE FOR BASIC STANDARDS provides the central basis within the United States of a complete and consistent system of physical measurement; coordinates that system with measurement systems of other nations; and furnishes essential services leading to accurate and uniform physical measurements throughout the Nation's scientific community, industry, and commerce. The Institute consists of a Center for Radiation Research, an Office of Measurement Services and the following divisions:

Applied Mathematics — Electricity — Mechanics — Heat — Optical Physics — Nuclear Sciences[2] — Applied Radiation[2] — Quantum Electronics[3] — Electromagnetics[3] — Time and Frequency[3] — Laboratory Astrophysics[3] — Cryogenics[3].

THE INSTITUTE FOR MATERIALS RESEARCH conducts materials research leading to improved methods of measurement, standards, and data on the properties of well-characterized materials needed by industry, commerce, educational institutions, and Government; provides advisory and research services to other Government agencies; and develops, produces, and distributes standard reference materials. The Institute consists of the Office of Standard Reference Materials and the following divisions:

Analytical Chemistry — Polymers — Metallurgy — Inorganic Materials — Reactor Radiation — Physical Chemistry.

THE INSTITUTE FOR APPLIED TECHNOLOGY provides technical services to promote the use of available technology and to facilitate technological innovation in industry and Government; cooperates with public and private organizations leading to the development of technological standards (including mandatory safety standards), codes and methods of test; and provides technical advice and services to Government agencies upon request. The Institute consists of a Center for Building Technology and the following divisions and offices:

Engineering and Product Standards — Weights and Measures — Invention and Innovation — Product Evaluation Technology — Electronic Technology — Technical Analysis — Measurement Engineering — Structures, Materials, and Life Safety[4] — Building Environment[4] — Technical Evaluation and Application[4] — Fire Technology.

THE INSTITUTE FOR COMPUTER SCIENCES AND TECHNOLOGY conducts research and provides technical services designed to aid Government agencies in improving cost effectiveness in the conduct of their programs through the selection, acquisition, and effective utilization of automatic data processing equipment; and serves as the principal focus within the executive branch for the development of Federal standards for automatic data processing equipment, techniques, and computer languages. The Institute consists of the following divisions:

Computer Services — Systems and Software — Computer Systems Engineering — Information Technology.

THE OFFICE FOR INFORMATION PROGRAMS promotes optimum dissemination and accessibility of scientific information generated within NBS and other agencies of the Federal Government; promotes the development of the National Standard Reference Data System and a system of information analysis centers dealing with the broader aspects of the National Measurement System; provides appropriate services to ensure that the NBS staff has optimum accessibility to the scientific information of the world. The Office consists of the following organizational units:

Office of Standard Reference Data — Office of Information Activities — Office of Technical Publications — Library — Office of International Relations.

---

[1] Headquarters and Laboratories at Gaithersburg, Maryland, unless otherwise noted; mailing address Washington, D.C. 20234.
[2] Part of the Center for Radiation Research.
[3] Located at Boulder, Colorado 80302.
[4] Part of the Center for Building Technology.

Molecular Beam Tube Frequency Biases Due To Distributed Cavity Phase Variations

Stephen Jarvis, Jr.

Time and Frequency Division
Institute for Basic Standards
U.S. National Bureau of Standards
Boulder, Colorado 80302

U.S. DEPARTMENT OF COMMERCE, Frederick B. Dent, Secretary

NATIONAL BUREAU OF STANDARDS, Richard W. Roberts, Director

Issued January 1975

Library of Congress Catalog Card Number: 74-600205

National Bureau of Standards Technical Note 660

Nat. Bur. Stand. (U.S.), Tech Note 660, 43 pages (Jan. 1975)
CODEN: NBTNAE

For sale by the Superintendent of Documents, U.S. Government Printing Office, Washington, D.C. 20402
(Order by SD Catalog No. C13.46:660) $1.00

CONTENTS

MOLECULAR BEAM TUBE FREQUENCY BIASES DUE TO DISTRIBUTED CAVITY PHASE VARIATIONS

For atomic beam frequency standards, an analysis is described for estimating the frequency bias due to distributed cavity phase difference over finite beam widths, and for estimating the resulting inaccuracy in power shift and beam reversal experiments. Calculated atomic trajectories and simplified rf-field distributions are used, as well as certain assumptions about beam tube alignment. The results are applied to one of the present NBS primary time & frequency standards and a shorter tube geometry.

One conclusion is that beam reversal experiments are not necessarily much more accurate than power shift experiments and that the use of both methods (plus the use of pulse techniques) is desirable.

Key words: Accuracy evaluation; Atomic beam frequency standards; Cavity phase shift.

I. INTRODUCTION

The primary sources of error in state-of-the-art Ramsey-type cesium beam frequency standards, which are approaching a part in 10^{13} accuracy, are the second-order Doppler shift (DS2) and the effect (PD) of a phase lead δ of the rf-field in the second cavity over the first.

An experimental method, based on the pulse technique [1,2,3] and theoretical methods using measured Ramsey resonance curves at different power levels [4,5], have been reported which predict the relevant velocity distribution $\rho(V)$ of detected atoms. From $\rho(V)$, it is an easy matter to compute pseudo-velocities $V_D(b, \nu_{MOD})$ and $V_P(b, \nu_{MOD})$ coefficients depending on the power parameter b and the modulation width for line-center servoing from which the biases due to DS2 and PD are:

$$\nu_{DS2} = -\Omega V_D^2(b, \nu_{MOD}), \qquad \left(\Omega \equiv \frac{\nu_{ces}}{2c^2}\right)$$

$$\nu_{PD} = -\frac{\delta}{2\pi L} V_P(b, \nu_{MOD}),$$

where ν_{ces} is the cesium transition frequency, c the speed of light, L is the cavity separation and ℓ the width of each cavity. Since $V_P/2\pi L$ is typically about 10 Hz/radian, a milliradian phase difference δ generates a bias ν_{PD} of $10^{-12}\nu_{ces}$. Even with careful cavity adjustment before assembly, control of δ to levels significantly lower than a milliradian is not at present practical, so that the value of δ obtained in the beam machine at any particular time must be inferred by other means. Two techniques are currently employed. In the first, the beam tube is designed to permit both forward and reversed beam operation. For forward operation, the bias is

$$\nu_B^F = \nu_{DS2}^F - \frac{\delta}{2\pi L} V_P^F + k^F,$$

where k^F is other sources of bias. For reversed operation, the bias is

$$\nu_B^R = \nu_{DS2}^R + \frac{\delta}{2\pi L} V_P^R + k^R.$$

(We must anticipate that (V_D, V_P) result from different velocity distributions in the two operating modes). The difference

$$\Delta_{FR} \equiv \nu_B^F - \nu_B^R$$

is found by comparison with a very stable source (its accuracy is irrelevant), and thus

$$\frac{\delta}{2\pi L} = - \frac{\Delta_{FR} - (\nu_{DS2}^F - \nu_{DS2}^R) - (k^F - k^R)}{V_P^F + V_P^R}$$

from which ν_{PD} is easily computed for each mode. For example,

$$\nu_B^F = \alpha (\Delta_{FR} + \nu_{DS2}^R + k^R) + (1-\alpha)(\nu_{DS2}^F + k^F),$$

where

$$\alpha = V_P^F / (V_P^F + V_P^R) \cong \frac{1}{2}.$$

This bias estimate is limited in accuracy by the measurement $\Delta_{FR}/2$, the average DS2 bias, and the (yet) unknown bias:

$$\frac{1}{2}(k^R + k^F).$$

In the second technique, two power levels are used, (b^1, b^2).

$$\nu_B^i = \nu_{DS2}^i - \frac{\delta}{2\pi L} V_P^i + k^i, \qquad (i = 1, 2).$$

(The velocity distributions may be slightly different for these cases; this must be considered in the calculation of the (V_D, V_P^i), or the two-velocity distribution approach used) [2]. Again, measuring:

$$\Delta_{12} \equiv \nu_R^1 - \nu_R^2 ,$$

we find:

$$\frac{\delta}{2\pi L} = - \frac{\Delta_{12} - (\nu_{DS2}^1 - \nu_{DS2}^2) - (h^1 - h^2)}{\nu_P^1 - \nu_P^2} .$$

Then:

$$\nu_B^1 = s\,(\Delta_{12} + \nu_{DS2}^2 + h^2) + (1-s)(\nu_{DS2}^1 + h^1),$$

where:

$$s = \nu_P^1 / (\nu_P^1 - \nu_P^2).$$

With care in the choice of power levels and sufficiently wide velocity distributions $|s|$ may be as small as about 3, but in any case, it will amplify the errors in Δ_{12}, ν_{DS2}, and h^i, by this factor. This method has the advantage of being applicable to any beam machine and of generating redundancy (for three or more power levels), but suffers from the amplification factor s. A combination of both methods (plus use of the pulse techniques) will be the best approach towards a comprehensive accuracy evaluation.

Our purpose in this paper is to estimate the amplification factor, s, and the (PV) bias h (b, ν_{MOD}), due to non-uniformity (phase variations) of the rf-field in the portions of the cavities traversed by the atomic beam. These effects must be expected to be the more important in accuracy evaluations the shorter the beam tube.

The estimate involves three components. In Section II, a ray-trace technique is described which is intended to model the beam tube under consideration and generates velocity distribution moments over the cavity windows. In Section III, a calculation is described which provides an estimate of the relevant rf-magnetic field in the microwave cavity with finitely conducting walls; only a simple

rectangular guide is considered. In Section IV, the atomic transition probability is derived, and the total bias computed for sinusoidal or squarewave modulation by averaging over the atomic beam.

In Section V, the application of these methods to specific systems is discussed.

II. RAY TRACING

Referring to figure 1, let $\rho = (Y_1, Z_1, Y_2, Z_2)$ be the parameter vector of atoms whose trajectories have coordinates (Y_1, Z_1) at the center of the first cavity, (Y_2, Z_2) at the second, where $\rho = 0$ is assumed to be on the line of centers of the cavity apertures. We consider those atoms with velocity V, and assume all trajectories make small angles with the line of centers. Let ω be the rf-field angular frequency, and let $P_{pq}(\rho, V, \omega)$ be the transition probability for one of these atoms over its passage through the two cavities and the uniform C-field region between the cavities.

Consider atoms emitted either "spin up" (j = 1) or "spin down" (j = 2). If transition occurs, these atoms contribute to the detector signal the flux element:

$$\rho_j^+(V, \rho)\, P_{pq}(\rho, V, \omega)\, d\rho\, dV,$$

$$(d\rho \equiv dY_1\, dZ_1\, dY_2\, dZ_2),$$

where $\rho_j^+ = 0$ if the path fails to pass from emitter to detector, and otherwise, ρ_j^+ is the emitter source strength, dependent on the position on the emitter face and the launch angles. If transition did not occur, the contribution to the detected flux element is:

$$\rho_j^-(V, \rho)\left(1 - P_{pq}(\rho, V, \omega)\right) d\rho\, dV,$$

where ρ_j^- has properties analogous to ρ_j^+.

Integrating over the cavity openings $\mathcal{R}(\rho)$ and the velocity, the total flux at the detector is:

$$g_D(\omega) = \int_c^\infty dV\, \rho_E(\rho, V) \int_{\mathcal{R}(\rho)} d\rho\, Q^*(V, \rho)\, P_{pq}(\rho, V, \omega)$$

neglecting a term independent of ω, and writing

$$\rho_E(\rho, V)\, Q^*(V, \rho) = \sum_{j=1}^{2} \left(\rho_j^+ - \rho_j^-\right),$$

where $\rho_E(p, V)$ is an emitter source strength and $Q^*(V, \not{p})$ a beam tube form function for unit source strength. (The Jacobian of the transformation from initial to final values of (Y, Z, $\dot{Y}$, $\dot{Z}$) through deflecting magnets where force is independent of X is unity.) For simplicity, we may take $\rho_E(p, V)$ to be the Maxwellian emission distribution, independent of $\not{p}$.

With the intention of expanding $P_{pq}(V, \omega)$ to second order in $\not{p}$, the ray trace computation generates the velocity dependent moments:

$$q_n(V) = \int_{\mathcal{R}(\not{p})} d\not{p}\, Q^*(V, \not{p}) \begin{pmatrix} 1 \\ Y_1 \\ Z_1 \\ Y_2 \\ Z_2 \\ Y_1^2 \\ Y_1 Z_1 \\ Z_1^2 \\ Y_2^2 \\ Y_2 Z_2 \\ Z_2^2 \\ Y_1 Y_2 \\ Y_1 Z_2 \\ Y_2 Z_1 \\ Y_2 Z_2 \end{pmatrix}$$

$(n = 1, 15)$

Finally, defining

$$\rho_n(V) = q_n(V)\, \rho_E(V),$$

we can write:

$$q_D(\omega) = \sum_{n=1}^{15} \int_0^\infty dV\, \rho_n(V)\, P^n_{pq}(\omega, V)$$

where P^n_{pq} are the appropriate expansion coefficients of $P_{pq}(p, V, \omega)$.

The computer program generates the $q_n(V)$ for several intervals ($m = 1, M$) in the detector plane, so that the effect of detector location may be studied.

III. THE CAVITY FIELD

The microwave structure is assumed to be a very symmetric U-shaped rectangular wave guide shorted at the ends and driven at the center. It propagates only the $TE_{0,1}$-mode, each arm having the ideal complex harmonic field structure

$$\mathbb{E}(\mathbb{r})e^{i\omega t} = \cos\frac{\pi z}{c_1}\sin\gamma_c(y+y_0)e^{i\omega t}\,\mathbb{K},$$

where $\mathbb{K}$ is a unit vector in the z-direction, γ_c is the cavity wave number and y_0 an arbitrary phase chosen to make $\mathbb{E}$ vanish at the short $y = -y_0$.

In beam machines, the apertures in the cavity arms which permit the atoms to pass through are usually elaborated with features which include transverse "approach sections" and horizontal (y-direction) fins to reduce field leakage in the x-direction. These complications make calculation of the exact rf field nearly impossible even in the case of perfectly conducting walls.

We have examined only the relatively simple case in which the cavity apertures are absent, and the wall conductivities are very high, dependant only on the perimeter position (independent of y). For the magnetic field-independent transition in cesium defining the atomic second, only the rf magnetic field parallel to the C-field, which we shall take in the z-direction, is important in causing transitions.

We shall solve the harmonic field equations:

$$\nabla\times\nabla\times\mathbb{E} - k^2\mathbb{E} = 0,$$

$$\mathbb{H} = -\frac{1}{i\omega\mu_c}\nabla\times\mathbb{E},$$

subject to the wall skin depth conditions

$$\mathbb{n}\times\mathbb{E} = \frac{1}{2}\delta(\mathbb{r}_s)\mu_w\omega(1+i)\mathbb{H}_T,$$

where $\mathbb{n}$ is the outward normal, $\delta(\mathbb{r}_s)$ the skin depth at the wall point $\mathbb{r}_s$ (independent of y), and $\mathbb{H}_T$ the tangential magnetic field on the wall. The wall condition can be written

$$\mathbb{n}\times\mathbb{E} = \epsilon(\mathbb{r}_s)(\nabla\times\mathbb{E})_T,$$

where:

$$\sigma(\nu_s) = \frac{i-1}{2}\,\delta(\nu_s),$$

where the real skin depth is

$$\delta(\nu_s) = \frac{\mu_w}{\mu_c}\sqrt{\frac{2}{\omega\mu_w\sigma_w(\nu_s)}}$$

$$\doteq 2.906(10)^{-2}\sqrt{\frac{\lambda_0}{\sigma}} \quad \text{cm.}$$

For $\sigma = 5.92 \times 10^5 \text{ohm}^{-1}\text{cm}^{-1}$ for copper, the free space cesium transition wave length $\lambda_0 = 3.264$ cm, we obtain:

$$\delta = 6.82(10)^{-5} \quad \text{cm}$$

Wave guide dimensions are assumed to be a = 2.286 cm (0.9") and b = 1.016 cm (0.4"). (X-band).

We take the electric field to be of the form

$$E_1(\nu) = \mathcal{E}_1(x,z)\sin\beta y,$$
$$E_2(\nu) = \mathcal{E}_2(x,z)\cos\beta y,$$
$$E_3(\nu) = \mathcal{E}_3(x,z)\sin\beta y;$$

$$\mathcal{E}_1(x,z) = (1+e_1(x))\cos\left[\left(\frac{\pi}{a}+\epsilon\right)z+\beta\right],$$
$$\mathcal{E}_2(x,z) = e_2(x)\cos\left[\left(\frac{\pi}{a}+\epsilon\right)z+\beta\right],$$
$$\mathcal{E}_3(x,z) = e_3(x)\sin\left[\left(\frac{\pi}{a}+\epsilon\right)z+\beta\right],$$

where the $e_j(z)$ are assumed to have series expansions in a mean skin depth $\bar{\delta}$, while ϵ and β are to be determined and are constants of order $\bar{\delta}$.

The important magnetic field component $H_3(\nu)$ is found to within a proportionality constant from:

$$H_3(\nu) = \sin\beta y\left\{e_{2,x}(x) + \beta(1+e_1(x))\right\}\cdot$$
$$\cdot\sin\left[\left(\frac{\pi}{a}+\epsilon\right)z+\beta\right].$$

The complex propagation constant $\gamma = \gamma_0 - i\alpha$ is determined by the analysis.

The calculation is extremely lengthy, and requires an analysis to second order in δ to determine all the first order quantities. It will not be reproduced here.

An end-short condition for terminal skin depth δ_e is easily applied to the result by replacing $\sin \delta y$ by $\sin \delta(y + y_0^{(\delta_e)})$ and applying one of the wall conditions at $y = -y_e$, which determines $y_0^{(\delta_e)}$. A second wall condition is ignored; in fact, the skin depth distribution must be of the correct form on the end wall to be consistent with this single mode analysis.

The real and imaginary parts of $H_3(\pi)$ are determined from a computer program where the primary input is constant values $(\delta_1, \delta_2, \delta_3, \delta_4, \delta_e)$ for the skin depths on the four walls and shorting surface. (In fact, the parametric variation of skin depth by cosine series coefficients is included, but such effects must be expected to be small; in any case, such coefficients are unknown).

Finally, coefficients of the real and imaginary parts of $H_3(\pi)$ are generated for least squares best fit to the form:

$$H_3(\pi) = \varphi_1(y,z) + x\,\varphi_2(y,z) + x^2\varphi_3(y,z),$$

$$\varphi_j(y,z) \equiv \varphi_1^j + \varphi_2^j y + \varphi_3^j z + \varphi_4^j y^2 + \varphi_5^j yz + \varphi_6^j z^2$$

about each cavity center $\pi = 0$ point on the line of centers of the cavity apertures. The program also gives the expansion coefficients for the remaining field components as well.

It must be emphasized that this relatively simple calculation may not represent adequately the true field in the complicated cavity structure near the cavity apertures, but we shall be able to determine which are the critical coefficients in the field expansion.

IV. THE TRANSITION PROBABILITY

The quantum mechanical probability amplitudes $C_1(t)$, $C_2(t)$ for a two-state system perturbed by a uniform magnetic field in the z-direction and a parallel oscillating field may be written:

$$i\begin{bmatrix}\dot{C}_1\\ \dot{C}_2\end{bmatrix} = \begin{bmatrix}E_1 & H_0\\ H_0 & E_2\end{bmatrix}\begin{bmatrix}C_1\\ C_2\end{bmatrix} + 2b\begin{bmatrix}0 & H_2\\ H_2 & 0\end{bmatrix}\begin{bmatrix}C_1\\ C_2\end{bmatrix},$$

where E_1, E_2 are the unperturbed frequencies associated with the energy states, H_0 a frequency associated with the uniform field, and b a constant proportional to the oscillating field amplitude (the "power parameter"). The field $H_2^j(\bar{r}, t)$ in each cavity $j = 1, 2$ is related to the complex field H_3^R, H_3^I calculated in Section III by:

$$H_2^j(\bar{r}, t) = \hat{\mu}_j\left[H_3^{jR}(\bar{r})\cos(\omega t + \chi_j) + H_3^{jI}(\bar{r})\sin(\omega t + \chi_j)\right],$$

where $\hat{\mu}_j$ and χ_j are chosen so that

$$H_2^j(\bar{r}, t) = -h_2^j(\bar{r})\cos(\omega t + \varphi_j) - h_1^j(\bar{r})\sin(\omega t + \varphi_j)$$

and:

$$h_1^j(0) = 1,$$
$$h_2^j(0) = 0.$$

We can readily compute from the coefficients for the field $(H_3^{jR}(\bar{r}), H_3^{jI}(\bar{r}))$ in Section III the representation

$$h_2^j(\bar{r}) = (c_1^j + c_2^j\bar{z} + c_3^j\bar{y} + c_4^j\bar{z}^2 + c_5^j\bar{z}\bar{y} + c_6^j\bar{y}^2) + \bar{x}(c_i^j \to c_{i+6}^j) + \bar{x}^2(c_i^j \to c_{i+12}^j),$$

in which $c_1^j = 0$. A similar expansion holds for h_1^j, but is not required.

We assume that the atom has a trajectory through each cavity:

$$\bar{x} = Vs,$$
$$\bar{y} = y + V_{y,x}s,$$
$$\bar{z} = z + V_{z,x}s,$$

where, assuming the atom enters the first cavity at time t = 0, $s = t - \frac{x}{2}$, in the first cavity, $s = t - (T + \frac{3}{2}\tau)$ in the second, with $\tau = \ell/V$, $T = L/V$. From the representation of the field components in terms of the c_n^s, we can express the time-dependent functions

$$\begin{bmatrix} b\, h_1^j(\omega(t)) \\ b\, h_2^j(\omega(t)) \end{bmatrix} = \begin{bmatrix} b \\ a \end{bmatrix} + \begin{bmatrix} \beta_{11}^j \\ \beta_{21}^j \end{bmatrix} + s \begin{bmatrix} \beta_{12}^j \\ \beta_{22}^j \end{bmatrix} + s^2 \begin{bmatrix} \beta_{13}^j \\ \beta_{23}^j \end{bmatrix}$$

$$\equiv \begin{bmatrix} b \\ a \end{bmatrix} + \begin{bmatrix} \mathcal{B}_1^j(s) \\ \mathcal{B}_2^j(s) \end{bmatrix},$$

where the coefficients β_{ij}^j are small, associated with the cavity resistivity and field amplitude gradients in each cavity.

The uniform field causes the energies of the states to be modified. The unitary diagonalizing matrix

$$A = \begin{bmatrix} \alpha H_0 & \alpha(\omega_1 - E_1) \\ \beta(\omega_2 - E_2) & \beta H_0 \end{bmatrix}$$

where:

$$\alpha = \frac{1}{\sqrt{(\omega_1 - E_1)^2 + H_0^2}}, \quad \beta = \frac{1}{\sqrt{(\omega_2 - E_2)^2 + H_0^2}},$$

$$\omega_{2,1} \equiv \frac{1}{2}(E_1 + E_2) \pm \sqrt{\frac{1}{4}(E_2 - E_1)^2 + H_0^2},$$

generates the following system for the eigenstates:

$$D \equiv A C,$$

$$i\begin{bmatrix} \dot{D}_1 \\ \dot{D}_2 \end{bmatrix} = \begin{bmatrix} \omega_1 & 0 \\ 0 & \omega_2 \end{bmatrix}\begin{bmatrix} D_1 \\ D_2 \end{bmatrix} + 2b\, A \begin{bmatrix} 0 & H_z \\ H_z & 0 \end{bmatrix} A^T \begin{bmatrix} D_1 \\ D_2 \end{bmatrix}.$$

For the very weak C-fields employed in beam machines, $H_0/(E_2 - E_1) \ll 1$, and A is essentially the unit matrix; the only important effect of H_0 is to replace (E_1, E_2) by (ω_1, ω_2). Thus, we consider only the system:

$$i\begin{bmatrix} \dot{D}_1 \\ \dot{D}_2 \end{bmatrix} = \begin{bmatrix} \omega_1 & 0 \\ 0 & \omega_2 \end{bmatrix}\begin{bmatrix} D_1 \\ D_2 \end{bmatrix} + 2b\begin{bmatrix} 0 & H_z \\ H_z & 0 \end{bmatrix}\begin{bmatrix} D_1 \\ D_2 \end{bmatrix}.$$

Putting:

$$D_1 = e^{-i\varphi_1} F_1,$$

$$D_2 = F_2,$$

which does not effect the state probabilities, (i.e., $|D_1^2| = |F_1^2|$):

$$i\begin{bmatrix} \dot{F}_1 \\ \dot{F}_2 \end{bmatrix} = \begin{bmatrix} \omega_1 - \dot{\varphi}_1 & 0 \\ 0 & \omega_2 \end{bmatrix}\begin{bmatrix} F_1 \\ F_2 \end{bmatrix} + 2h\begin{bmatrix} 0 & H_2 e^{i\varphi_1} \\ H_2 e^{-i\varphi_1} & 0 \end{bmatrix}\begin{bmatrix} F_1 \\ F_2 \end{bmatrix}.$$

Introducing in the j^{th} cavity (j = 1, 2),

$$H_2^j(\pi(t)) = -h_2^j \cos(\omega t + \varphi_j) - h_1^j \sin(\omega t + \varphi_j),$$

and putting:

$$\varphi_1(t) = -\omega t - \varphi_2, \quad \delta_j \equiv \varphi_2 - \varphi_j;$$

$$i\begin{bmatrix} \dot{F}_1 \\ \dot{F}_2 \end{bmatrix} = \begin{bmatrix} (\omega_1 + \omega) F_1 - b(h_2^j - i h_1^j) e^{-i\delta_j} F_2 \\ -b(h_2^j + i h_1^j) e^{i\delta_j} F_1 + \omega_2 F_2 \end{bmatrix} + \mathcal{E},$$

where $\mathcal{E}$ is composed of terms with oscillating frequency 2ω. These lead to the Bloch-Siegert Shift [6], which we shall not consider here.

We introduce the real variables:

$$U = F_1 \tilde{F}_1, \quad V = F_2 \tilde{F}_2, \quad R = F_1 \tilde{F}_2 + F_2 \tilde{F}_1, \quad S = -i(F_1 \tilde{F}_2 - F_2 \tilde{F}_1);$$

$$U + V = 1, \quad W \equiv U - V; \quad U = \frac{1}{2}(1 + W), \quad V = \frac{1}{2}(1 - W);$$

and derive the real equations

$$\dot{W} = 2b R(h_1^j \cos\delta_j + h_2^j \sin\delta_j) + 2b S(h_2^j \cos\delta_j - h_1^j \sin\delta_j),$$

$$\dot{R} = \lambda S - 2b W(h_1^j \cos\delta_j + h_2^j \sin\delta_j),$$

$$\dot{S} = -\lambda R - 2b W(h_2^j \cos\delta_j - h_1^j \sin\delta_j),$$

where

$$\lambda \equiv \omega - \omega_c, \quad \omega_c \equiv \sqrt{\omega_0^2 + 4H_0^2}, \quad \omega_0 = E_2 - E_1.$$

(The sign of λ is reversed from Ramsey's [7] usage). The effect of $\delta_j \neq 0$ is merely a rotation in the (R, S) subspace. With the initial data at t = 0:

$$|C_p^2| = U = 1, \quad V = R = S = 0,$$

so that W = 1, we can write after passage throught the first cavity:

$$\begin{bmatrix} W' \\ R \\ S \end{bmatrix}_\tau = \begin{bmatrix} 1 & 0 & 0 \\ 0 & \cos\delta & \sin\delta \\ 0 & -\sin\delta & \cos\delta \end{bmatrix} \mathcal{H}^1 \begin{bmatrix} 1 \\ 0 \\ 0 \end{bmatrix}_0 \qquad \delta \equiv \delta_2 - \delta_1 ,$$

where H' satisfies:

$$\begin{bmatrix} W' \\ R \\ S \end{bmatrix}_\tau = \mathcal{H}^1 \begin{bmatrix} W \\ R \\ S \end{bmatrix}_0$$

over cavity one with $\delta_1 = 0$. Over the C-field region, b = 0, we have:

$$\begin{bmatrix} W' \\ R \\ S \end{bmatrix}_{T+\tau} = \begin{bmatrix} 1 & 0 & 0 \\ 0 & \cos\lambda T & \sin\lambda T \\ 0 & -\sin\lambda T & \cos\lambda T \end{bmatrix} \begin{bmatrix} W \\ R \\ S \end{bmatrix}_\tau .$$

Over the second cavity, we have ($\delta_2 = 0$):

$$\begin{bmatrix} W \\ R \\ S \end{bmatrix}_{T+2\tau} = \mathcal{H}^2 \begin{bmatrix} W \\ R \\ S \end{bmatrix}_{T+\tau}$$

We need finally the transition probability at $t = T + 2\tau$:

$$P_{pq} = |C_q^2| = V(T+2\tau) = \tfrac{1}{2}(1 - W(T+2\tau)).$$

Then:

$$W(T+2\tau) = \begin{bmatrix} 1 & 0 & 0 \end{bmatrix} \mathcal{H}^2 \begin{bmatrix} 1 & 0 & 0 \\ 0 & \cos(\lambda T+\delta) & \sin(\lambda T+\delta) \\ 0 & -\sin(\lambda T+\delta) & \cos(\lambda T+\delta) \end{bmatrix} \mathcal{H}^1 \begin{bmatrix} 1 \\ 0 \\ 0 \end{bmatrix}.$$

The cavity equations may be written:

$$\dot{W} - 2bR = 2\beta_1^j R + 2\beta_2^j S,$$

$$\dot{R} + \lambda S + 2bW = -2\beta_1^j W,$$

$$\dot{S} + \lambda S = -2\beta_2^j W.$$

If this sytem is iterated once, treating the right-hand-side as a small perturbation, we can write for cavity j:

$$\mathcal{H}^j = \mathcal{H}^c + \mathcal{J}^j$$

where the matrix $\mathcal{H}^0$ is the same for each cavity, and I^j is a small perturbation matrix. With $a = \sqrt{\lambda^2 + 4b^2}$,

$$\mathcal{H}^c = \frac{1}{2a^2} \begin{pmatrix} 2(\lambda^2 + 4b^2 \cos at) & 4ab \sin at & 4\lambda b(1 - \cos at) \\ -4ab \sin at & \cdot & \cdot \\ 4\lambda b(1 - \cos at) & \cdot & \cdot \end{pmatrix}$$

Then to the first order in I^j, the transistion probability is found from:

$$1 - 2P_{pq} = (\mathcal{H}^c_{11})^2 + \mathcal{H}^c_{11}(\delta'_{11} + \delta^2_{11})$$
$$+ \cos(\lambda T + \delta)(\mathcal{H}^c_{12}\mathcal{H}^c_{21} + \mathcal{H}^c_{12}\delta'_{21} + \mathcal{H}^c_{21}\delta^2_{12} + \mathcal{H}^c_{13}\mathcal{H}^c_{31} + \mathcal{H}^c_{13}\delta'_{31} + \mathcal{H}^c_{31}\delta^2_{13})$$
$$+ \sin(\lambda T + \delta)(\mathcal{H}^c_{12}\mathcal{H}^c_{31} + \mathcal{H}^c_{12}\delta'_{31} + \mathcal{H}^c_{31}\delta^2_{12} - \mathcal{H}^c_{13}\mathcal{H}^c_{21} - \mathcal{H}^c_{13}\delta'_{21} - \mathcal{H}^c_{21}\delta^2_{13}).$$

Line centering by the modulation technique is modeled by putting

$$\lambda \rightarrow \lambda^* + \lambda_{MOD}\, p(t)$$

where p(t) is a symmetric periodic function, usually a square-wave or a sinusoidal wave, λ_{MOD} is a modulation amplitude and λ^* is a small adjustable offset. λ^* is varied so that the detector signal is also a symmetric periodic function as sensed by a symmetric linear filter. Assuming that δ, I, and λ^* are all small quantities, the asymmetric part of P_{pq} is as follows:

($\lambda = \lambda_{MOD}$ here):

$$-2\overset{o}{P}_{pq}(\lambda) = \mathcal{H}^c_{11}(\overset{o}{\delta}'_{11} + \overset{o}{\delta}^2_{11}) + 2\lambda^* \mathcal{H}^c_{11}\mathcal{H}^c_{11,\lambda}$$
$$+ \cos\lambda T\{(\lambda^* T + \delta) \cdot 2\mathcal{H}^c_{12}\mathcal{H}^c_{31}$$
$$+ 2\lambda^*(\mathcal{H}^c_{12}\mathcal{H}^c_{21,\lambda} + \mathcal{H}^c_{13}\mathcal{H}^c_{31,\lambda})$$
$$+ \mathcal{H}^c_{12}(\overset{o}{\delta}'_{21} - \overset{o}{\delta}^2_{12}) + \mathcal{H}^c_{13}(\overset{E}{\delta}'_{31} + \overset{E}{\delta}^2_{13})\} \longrightarrow$$

$$+ \sin\lambda T \Big\{ (\lambda^* T + S)(\mathcal{H}^c_{,2})^2 + 2\lambda^* (\mathcal{H}^c_{,2}\mathcal{H}^c_{31,\lambda} + \mathcal{H}^c_{12,\lambda}\mathcal{H}^c_{3,1}) + \mathcal{H}^c_{,2}(\overset{=}{\mathcal{D}}{}^1_{31} + \overset{=}{\mathcal{D}}{}^2_{13}) - \mathcal{H}^c_{,3}(\mathcal{D}^1_{21} - \mathcal{D}^2_{12}) \Big\},$$

where (O, E) refer to antisymmetric and symmetric parts in λ_{MOD}, respectively.

We also assume a modulation amplitude small enough that terms in $(\lambda_{MOD}/b)^2$ may be ignored. To this order, we calculate:

$$\mathcal{Q}^j = \begin{pmatrix} \frac{\lambda}{b}(\mathcal{C}^j_5 - \mathcal{C}^j_3) & -\frac{\lambda}{b}\mathcal{C}^j_{10} & 2\mathcal{C}^j_5 \\ -\frac{\lambda}{b}\mathcal{C}^j_{14} & \cdot & \cdot \\ -2\mathcal{C}^j_3 & \cdot & \cdot \end{pmatrix}$$

where in each cavity j:

$$\begin{pmatrix} \mathcal{C}^j_3 \\ \mathcal{C}^j_5 \\ \mathcal{C}^j_{10} \\ \mathcal{C}^j_{14} \end{pmatrix} = \sum_{K=1}^{3} \begin{pmatrix} \tau^K \beta_{2K}\, \gamma_{1K} \\ \tau^K \beta_{2K}(\cos 2b\tau \cdot \gamma_{1K} + \sin 2b\tau\, \gamma_{2K}) \\ \tau^K \beta_{2K}\, \gamma_{2K} \\ \tau^K \beta_{2K}(\sin 2b\tau \cdot \gamma_{1K} - \cos 2b\tau \cdot \gamma_{2K}) \end{pmatrix},$$

and

$$\tau^K \gamma_{iK} = \int_{-\frac{\tau}{2}}^{\frac{\tau}{2}} ds \begin{pmatrix} \cos 2b(s+\frac{\tau}{2}) \\ \sin 2b(s+\frac{\tau}{2}) \\ \cos^2 2b(s+\frac{\tau}{2}) \\ \frac{1}{2}\sin 4b(s+\frac{\tau}{2}) \end{pmatrix}_i \begin{pmatrix} 1 \\ s \\ s^2 \end{pmatrix}_K ; \qquad \begin{matrix} (i = 1, \ldots, 4 \\ K = 1, 2, 3) \end{matrix}$$

The frequency bias ν_B and the second order Doppler correction are introduced by writing:

$$\lambda^* = 2\pi(\nu_B + \Omega V^2).$$

Then integrating P_{pq} over velocity and the permissible atom trajectories, and carrying out the linear filtering associated with modulation, a null result is obtained when the frequency bias ν_B satisfies:

$$0 = \nu_B\, u_1 + \Omega\, u_2 + \frac{\delta}{2\pi L}\, u_3 + \sum_{k=1}^{18} \left(c_k^1\, u_{k+3} + c_k^2\, u_{k+21} \right),$$

where the C_k^j are the $h_2^j(\vec{r})$ expansion coefficients for cavities j = (1, 2), and the $u_j(b, \nu_{MOD})$ are defined in the Appendix.

Calling

$$v_k(b, \nu_{MOD}) \equiv u_{k+1} / u_1, \qquad (k = 1, \ldots, 17),$$

we obtain for the bias:

$$\nu_B = -\Omega\, v_1 - \frac{\delta}{2\pi L}\, v_2 - \left\{ \sum_{k=1}^{17} \left(c_k^1\, v_{k+2} + c_k^2\, v_{k+20} \right) \right\},$$

where we can now identify the terms used in the discussion of bias estimation in Section I:

$$\nu_{DP2} = -\Omega\, v_1, \qquad v_1 = V_D^2,$$

$$V_P = v_2,$$

and $(-h)$ is the bracketed term.

A computer program has been written which accepts the velocity distributions $q_n^m(V)$ of Section II, the H-field coefficients $\{\varphi_n\}$ of Section III, a set of field level parameters $\{b\}$, and a single modulation frequency width ν_{MOD}. For each detector location m, it computes the $v_k(b, \nu_{MOD})$, and taking pairs of field coefficient sets, constructs the associated constants c_k^j. It presents the PV bias $h(b)$, and for pairs (b_1, b_2), presents the power shift error multipliers of the coefficients (c_k^1, c_k^2) as well as the power shift-induced error for that field pair.

V. APPLICATIONS

The procedures described here have been applied to two systems, NBS-5 and a shorter off-line beam tube (Tube B). However, it must be born in mind that the NBS-5 results are relevant to the true system only if two assumptions hold. First, the ray trace must adequately match the system. This may be checked reasonably well for $\rho_1(V)$ which is just the detected velocity distribution, but not at all for the other distributions ($\rho_2, \ldots, \rho_{15}$) which are much more critically dependent on system and cavity alignment. Second, the simple wave guide model must be adequate to represent the complicated structure of the cavity apertures. For a given structure, however, if all skin depths are increased by a factor x, then all σ_n^j, and hence the PV bias Δ, are increased by the factor x. Skin depths are expected to be known to (and have a time-dependent change of) only a few percent.

We have considered only three rf-field types. In the first, the skin depth is uniformly 6.82×10^{-5} cm, corresponding to copper. In the second, skin depths are uniformly 10% higher, while in the third, only two adjacent walls are 10% higher, which should represent a worst case for non-uniformity in this simple model.

Figure 2 shows the correct velocity distribution for NBS-5, as determined by measurement and confirmed by Ramsey curve inversion. Also shown are ray trace results for a detector of height 0.2 cm, centered 0.3 cm below the line of centers for M= 2, 0.3 cm above the line of centers for M = 4. All these curves are normalized to unit height. Neither ray trace curve matches the experimental curve well; the M = 2 curve has a better center of gravity, while the M = 4 curve has the proper location for the maximum. These ray traces were done directly from the beam tube design value, and no effort was made to adjust them to improve the match.

Figure 3 shows results for an off-line geometry with an interaction region length L = 0.5m. Both detectors, M = 1 and M = 3, are located on the opposite side of the line of centers from the emitter, with the M = 1 detector further away. The strongest signal is detected at the M = 3 location, while the M = 1 is very weak, and exhibits "shot noise" of the limited number of rays examined.

In table 1 we list the most important rf-field expansion coefficients c_n and field derivative at $\bar{r} = 0$ which they represent for the three rf-field types we have examined. In table 2, we show the corresponding multipliers (c_{n+2}, c_{n+20}) for the two cavity fields at nominal modulation amplitude (equal to resonance half-width) for three values of b bracketing the optimum value. When the field type is assigned to each cavity (j = 1, 2), each product $c_n^j c_{n+2}$, $c_n^j c_{n+20}$ is a component of the PV bias $h(b, \nu_{MOD})$. K = 1 for the NBS-5 model; K = 2 for the shorter tube (Tube B). S = 1 is when the beam tube geometry is completely symmetric about y = 0; S = 2 is the case in which emitter and detector are shifted 0.1 cm on opposite sides of the symmetry axis y = 0, and show the effect of misalignment. (A similar effect is produced by non-uniform emission or detection in y). M is the particular detector location number (varied in z).

Referring to c_2 (∂_z), even though c_4 and c_{22} may be quite large, as long as the cavity aperture is centered (in z) in the wave guide face and the z-dimension of the cavity opening (here 0.95 for K = 1, 0.508 for K = 2) is not too large, this term is not important.

Referring to C_3 (∂_y), we see that the unavoidable rf-field phase gradient in the propagating direction can be a major source of PV bias for relatively small beam asymmetries in y, whether due to physical misalignment of components or non-uniform beam intensity. The values (c_5, c_{23}) for K = (1, 2) appear to be roughly proportional to the slope $y_{,x}$ of the misalignment assumed. This error can be reduced by narrowing the cavity aperture widths (here 1.27 cm) at a proportionate loss in detected signal.

The field curvature terms (c_4, c_6) are in the 1×10^{-4} range for K = 1, but as high as 2×10^{-3} for the shorter tube. These terms should drop quadratically with decreasing aperture dimensions.

The terms due to C_7 and C_{13} which modify the transition probability by introducing an apparent frequency variation in the cavity have very substantial coefficients, (c_9, c_{16}) and (c_{27}, c_{33}), for the two cavities, but are fortunately of such amplitudes and signs as to cancel identically when the cavities and their fields are identical. For the variations in cavity fields considered here, these terms are less than 1×10^{-4}, but x-asymmetries in cavity construction could perhaps produce large biases because of these terms. It is worth

noting, however, that the (σ_9, σ_{16}, σ_{33}) depend only on $\rho_1(V)$ the directly determinable velocity distribution; in a cavity design in which these biases were dominant, power shift measurements could be used to estimate (C_4, C_6), and some correction applied.

Tables 3 through 10 are final results for these cases. Over a set of relevant power parameter values $\{b\}$, V_D and $V_p(b, \nu_{MOD})$ are shown; these numbers are independent of which rf-field types are used. For the cavity 1/cavity 2 rf-field type designations shown, the PV bias h is given, and for power parameter pairs, (b^+, b^-), the resulting PV power-shift bias

$$\nu_B^{PV} \equiv \alpha\, h(b^+, \nu_{MOD}) + (1-\alpha)\, h(b^-, \nu_{MOD}),$$

due only to distribution of phase over cavity-apertures, is given in Hertz. (For cesium, a 1.0×10^{-3} Hz bias is approximately 1 part in 10^{13}). These numbers can be considered to represent the uncertainty values which are encountered under the conditions stated.

Let us now consider a few specific examples. Consider the case of NBS-5 (K=1) operated between $b^- = 20000\ s^{-1}$ (near optimum for M = 4) and $b^+ = 2\ b^{-1}$ (6 dB higher power). With perfect symmetry in y (S = 1; tables 3 and 4), we find PV power shift biases of 0.6×10^{-3} Hz for M = 2 and 0.4×10^{-3} Hz for M = 4. The corresponding PV beam reversal biases, $1/2(h^F + h^R)$, at b^- are 0.2×10^{-3} Hz for M = 2 and 0.0×10^{-3} Hz for M = 4.

For the asymmetric case (S = 2; tables 5 and 6), the PV power shift biases are 1.1×10^{-3} Hz for M = 2, and 1.0×10^{-3} Hz for M = 4. The corresponding PV beam reversal biases at b^- are 0.8×10^{-3} Hz for M = 2 and 0.6×10^{-3} Hz for M = 4.

We should remember that these biases do not include the DS2 bias (which can be very accurately calculated), and must be considered to be uncorrectable uncertainties at this time.

Consider now the shorter Tube B (K = 2) operated between $b^- = 14000\ s^{-1}$ (near optimum for M = 3) and $b^+ = 23000\ s^{-1}$, (4.3 db higher power). With perfect symmetry in y (S = 1: Tables 7 and 8),we find PV power shift biases of $25. \times 10^{-3}$ Hz for M = 1 and 2.5×10^{-3} Hz for M = 3, a very striking difference. The corresponding PV beam reversal-biases at b^- are 0.8×10^{-3} Hz for M = 1 and 0.5×10^{-3} Hz for M = 3.

For the asymmetric case (S = 2; tables 9 and 10), the PV power shift biases are 17×10^{-3} Hz for M = 1 and 3.0×10^{-3} Hz for M = 3. The corresponding PV beam reversal biases are 5.8×10^{-3} Hz for M =1 and 2.8×10^{-3} Hz for M = 3.

It is interesting to note that the power shift results are not always as bad relative to the beam reversal results as might have been expected from the values of the amplification factors $\mathcal{A}$ which are easily computed from the $V_p(b)$ values in the respective cases: for NBS-5 (K=1), $\mathcal{A} = 5$ for M = 2, and $\mathcal{A} = 9$ for M = 4, while for Tube B (K = 2), $\mathcal{A} = 13$ for M = 1 and M = 3. This is due to the high degree of correlation of PV biases at various power levels for a fixed configuration.

VI. CONCLUSIONS

Under rather severe assumptions on cavity symmetry and ray-tracing validity, estimates of the PV bias uncertainty (due to distributed field phase and amplitude in the cavities) have been obtained for power shift measurements on NBS-5 and a shorter beam tube, and tabulated in tables 3 through 10. With proper care in alignment and emitter fabrication, and optimum

choice of power levels, the PV bias uncertainty in power shift experiments with NBS-5 should be less than $1 \times 10^{-13} \nu_{ces}$.

It is important to note from these tables that the apparent advantage of beam reversal techniques may be substantially negated because of the fact that, in beam reversal, we must average two uncorrelated PV biases $\mathcal{k}^1$ and $\mathcal{k}^2$, while for power shift measurements, even though the amplification factor $\mathcal{s}$ may exceed 3, the biases $\mathcal{k}^1$ and $\mathcal{k}^2$ are correlated, and the resulting bias uncertainty may even be less than the average $(\mathcal{k}^1 + \mathcal{k}^2)/2$. This fact confirms the view that a combination of both methods (plus the use of pulse techniques) is the best approach toward a comprehensive accuracy evaluation.

VII. APPENDIX

With $z = 2\pi L\, \nu_{MOD}/V$, we define the linear servo filter:

$$\mathcal{L}_t \begin{bmatrix} \sin \lambda T \\ \lambda T \cos \lambda T \\ \lambda T \end{bmatrix} = \begin{bmatrix} J_1(z) \\ J_2(z) \\ J_3(z) \end{bmatrix},$$

over $\lambda(t) = \lambda_{MOD}\, p(t)$. For square-wave modulation:

$$\mathcal{L}_t\left[F(\lambda T)\right] \equiv F(z); \quad \left\{ \begin{array}{l} J_1(z) = \sin z \\ J_2(z) = z \cos z \\ J_3(z) = z. \end{array} \right\}.$$

For sinusoidal modulation,

$$\mathcal{L}_t\left[F(\lambda T)\right] = \frac{\omega_M}{2\pi} \int_0^{\frac{2\pi}{\omega_M}} dt \sin \omega_M t\, F(\lambda_{MOD} \sin \omega_M t),$$

$$\left\{ \begin{array}{l} J_1(z) = J_1(z) \\ J_2(z) = z J_0(z) - J_1(z) \\ J_3(z) = \frac{1}{2} z \end{array} \right\},$$

where J_0, J_1 are Bessel functions.

With $x = b\tau$, we define

$$\mathcal{A}_{1K} \equiv \frac{2}{L} J_3(z) \frac{\cos 2x}{x}\left[\gamma_{1K}(\cos 2x - 1) + \gamma_{2K} \sin 2x \right]$$

$$\mathcal{A}_{2K} \equiv -2 J_1(z) \sin 2x\, \gamma_{1K} + \frac{2}{L} J_2(z) \cdot \left[\frac{\sin 2x}{x} \gamma_{2K} + \frac{1 - \cos 2x}{x}(\cos 2x\, \gamma_{1K} + \sin 2x\, \gamma_{2K}) \right]$$

Then we define the $\mathcal{C}_j(b, \nu_{MOD}, V)$:

$$\mathcal{C}_1 = \sin^2 2x\, J_1 + \frac{2}{L} \frac{\sin 2x}{x}(1 - \cos 2x)(J_1 + J_2),$$

$$\mathcal{C}_2 = \sin^2 2x\, J_1 + \frac{2}{L} \frac{\sin 2x}{x}(1 - \cos 2x) J_2,$$

$$\mathcal{C}_3 = -\mathcal{C}_0 = \mathcal{A}_{21} x / 2\pi L,$$

$$a_4 = a_7 = (t_{12} + t_{22})\, x/2\pi L ,$$

$$a_5 = -a_8 = t_{23}\, x/2\pi L .$$

where we have dropped the terms of order $(\ell/L)^2$.

Then designating:

$$\langle F(V) \rangle \equiv \int_0^\infty dV\, F(V),$$

the $u_i(b, \nu_{MOD})$ are as follows:

$$u_1 = \langle a_1 \rho_1 / V \rangle , \quad u_2 = \langle a_1 \rho_1 V \rangle , \quad u_3 = \langle a_2 \rho_1 \rangle$$

$$u_4 = \langle a_3 \rho_1 \rangle , \quad u_5 = \langle a_3 \rho_3 + \frac{\ell}{L} a_4 (\rho_5 - \rho_3) \rangle$$

$$u_6 = \langle a_3 \rho_2 + \frac{\ell}{L} a_4 (\rho_4 - \rho_2) \rangle$$

$$u_7 = \langle a_3 \rho_5 + 2 \frac{\ell}{L} a_4 (\rho_{15} - \rho_8) \rangle$$

$$u_8 = \langle a_3 \rho_7 + \frac{\ell}{L} a_4 (\rho_{14} + \rho_{13} - 2\rho_7) \rangle$$

$$u_9 = \langle a_3 \rho_6 + \frac{\ell}{L} a_4 (\rho_{12} - \rho_6) \rangle$$

$$u_{10} = \ell \langle a_4 \rho_1 \rangle$$

$$u_{11} = \ell \langle a_4 \rho_3 + \frac{\ell}{L} a_5 (\rho_5 - \rho_3) \rangle$$

$$u_{12} = \ell \langle a_4 \rho_2 + \frac{\ell}{L} a_5 (\rho_4 - \rho_2) \rangle$$

$$u_{13} = \ell \langle a_4 \rho_8 + 2 \frac{\ell}{L} a_5 (\rho_{15} - \rho_8) \rangle$$

$$u_{14} = \ell \langle a_4 \rho_7 + \frac{\ell}{L} a_5 (\rho_{14} + \rho_{13} - 2\rho_7) \rangle$$

$$u_{15} = \ell \langle a_4 \rho_6 + 2 \frac{\ell}{L} a_5 (\rho_{12} - \rho_6) \rangle$$

$$u_{16} = \ell^2 \langle a_5 \rho_1 \rangle , \quad u_{17} = \ell^2 \langle a_5 \rho_3 \rangle$$

$$u_{18} = \ell^2 \langle a_5 \rho_2 \rangle , \quad u_{19} = \ell^2 \langle a_5 \rho_5 \rangle$$

$$u_{20} = \ell^2 \langle a_5 \rho_7 \rangle , \quad u_{21} = \ell^2 \langle a_5 \rho_6 \rangle$$

$$u_{22} = \langle a_6 \rho_1 \rangle , \quad u_{23} = \langle a_6 \rho_5 + \frac{\ell}{L} a_7 (\rho_5 - \rho_3) \rangle$$

$$u_{24} = \langle a_6 \rho_4 + \frac{\ell}{L} a_7 (\rho_4 - \rho_2) \rangle$$

$$u_{25} = \langle a_6 \rho_{11} + 2 \frac{\ell}{L} a_7 (\rho_{11} - \rho_{15}) \rangle$$

$$u_{26} = \langle a_6 \rho_{10} + \frac{\ell}{L} a_7 (2\rho_{10} - \rho_{13} - \rho_{14}) \rangle$$

$$u_{27} = \langle a_6 \rho_9 + 2\frac{\ell}{L} a_7 (\rho_9 - \rho_{12}) \rangle$$

$$u_{28} = \ell \langle a_7 \rho_1 \rangle$$

$$u_{29} = \ell \langle a_7 \rho_5 + \frac{\ell}{L} a_8 (\rho_5 - \rho_3) \rangle$$

$$u_{30} = \ell \langle a_7 \rho_4 + \frac{\ell}{L} a_8 (\rho_4 - \rho_2) \rangle$$

$$u_{31} = \ell \langle a_7 \rho_{11} + 2\frac{\ell}{L} a_8 (\rho_{11} - \rho_{15}) \rangle$$

$$u_{32} = \ell \langle a_7 \rho_{10} + \frac{\ell}{L} a_8 (2\rho_{10} - \rho_{13} - \rho_{14}) \rangle$$

$$u_{33} = \ell \langle a_7 \rho_9 + 2\frac{\ell}{L} a_8 (\rho_9 - \rho_{12}) \rangle$$

$$u_{34} = \ell^2 \langle a_8 \rho_1 \rangle, \quad u_{35} = \ell^2 \langle a_8 \rho_5 \rangle$$

$$u_{36} = \ell^2 \langle a_8 \rho_4 \rangle, \quad u_{37} = \ell^2 \langle a_8 \rho_{11} \rangle$$

$$u_{38} = \ell^2 \langle a_8 \rho_{10} \rangle, \quad u_{39} = \ell^2 \langle a_8 \rho_9 \rangle$$

VIII. REFERENCES

1. Hellwig, H., Jarvis, S., Glaze, D. J., Halford, D., Bell, H. E., "Time Domain Velocity Selection Modulation as a Tool to Evaluate Cesium Beam Tubes", Proc. 27th Annual Frequency Control Symp., Ft. Monmouth, pp. 357-366, (1973).

2. Howe, D. A., Bell, H. E., Hellwig, H., DeMarchi, A., "Preliminary Research and Development of the Cesium Tube Accuracy Evaluation System," 28th Annual Symposium on Frequency Control, 1974.

3. Glaze, D. J., Hellwig, H., Allan, D. W., Jarvis, S. Jr., Wainwright, A. E., Bell, H. E., "Accuracy Evaluation and Stability of the NBS Primary Frequency Standards, IEEE Transactions on Instrumentation and Measurement, IM-23, 1974.

4. Jarvis, S. Jr., "Determination of Velocity Distributions in Molecular Beam Frequency Standards," Metrologia, 10, 3, pp. 87-98, September, 1974.

5. Daams, H., "Corrections for Second Order Doppler Shift and Cavity Phase Error in Cesium Atomic Beam Frequency Standards," IEEE Transactions on Instrumentation and Measurements, IM-23, 1974.

6. Shirley, J.H., "Some Causes of Resonant Frequency Shifts in Atomic Beam Machines," J. Appl. Phys., 34, 4, 783-788, April, 1963.

7. Ramsey, N.F., "Molecular Beams," Oxford University Press, London, 1956.

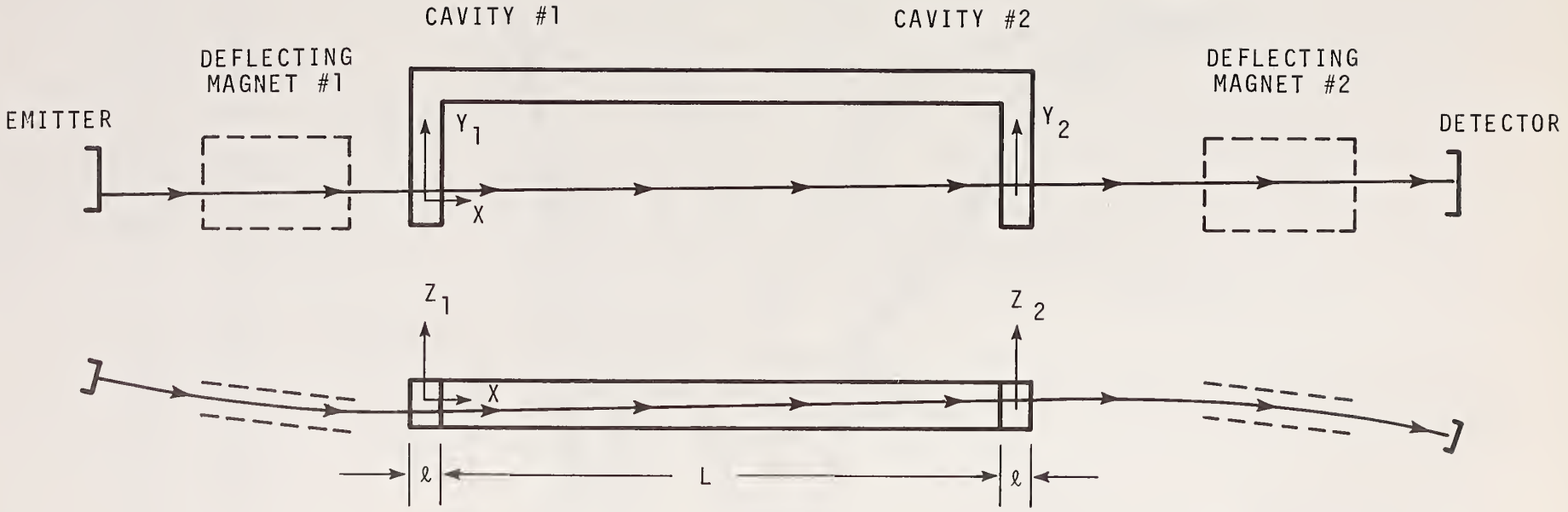

FIGURE 1: Schematic Diagram of Beam Tube Geometry

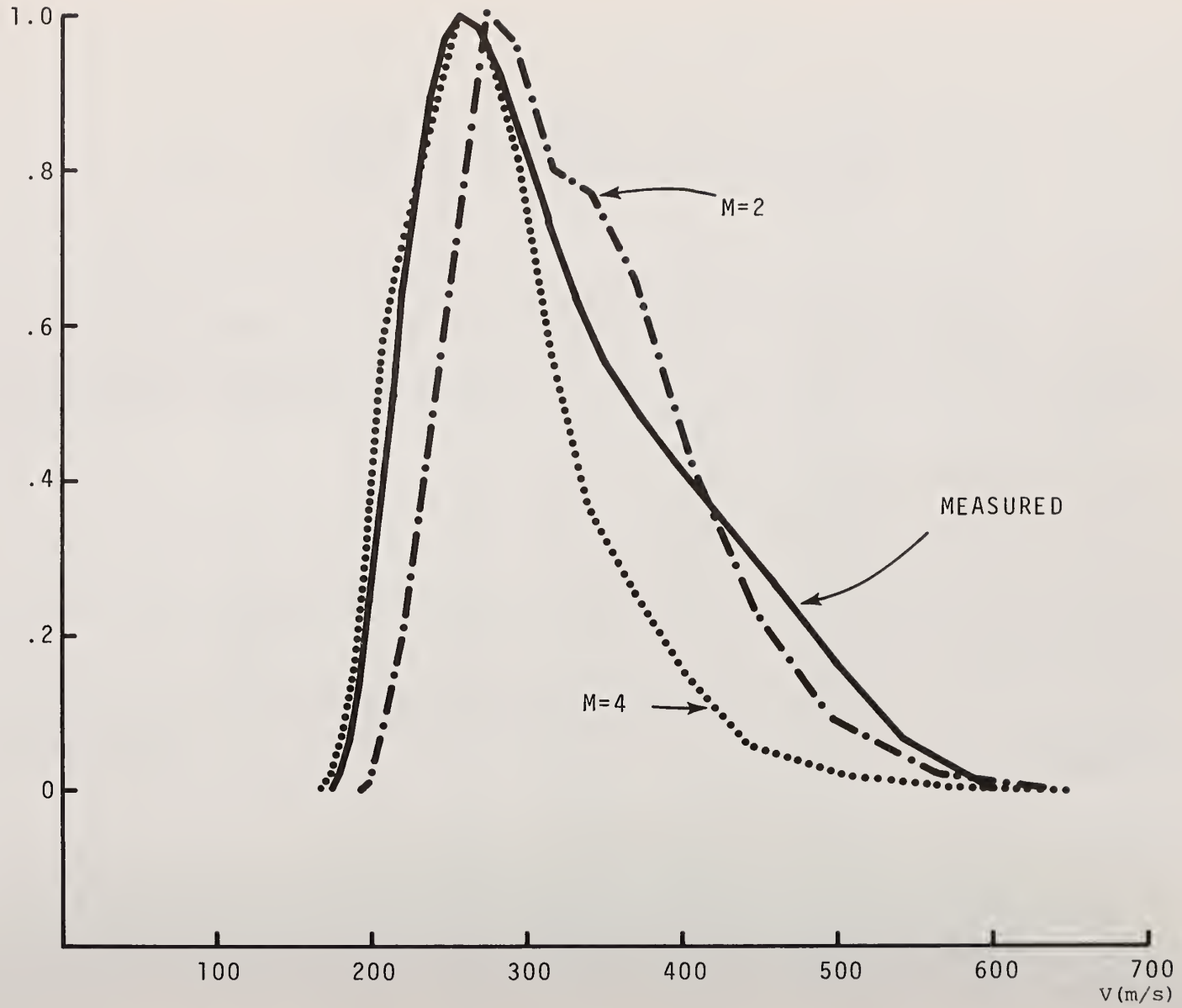

FIGURE 2: Measured and Simulated Velocity Distributions (normalized) for NBS-5.

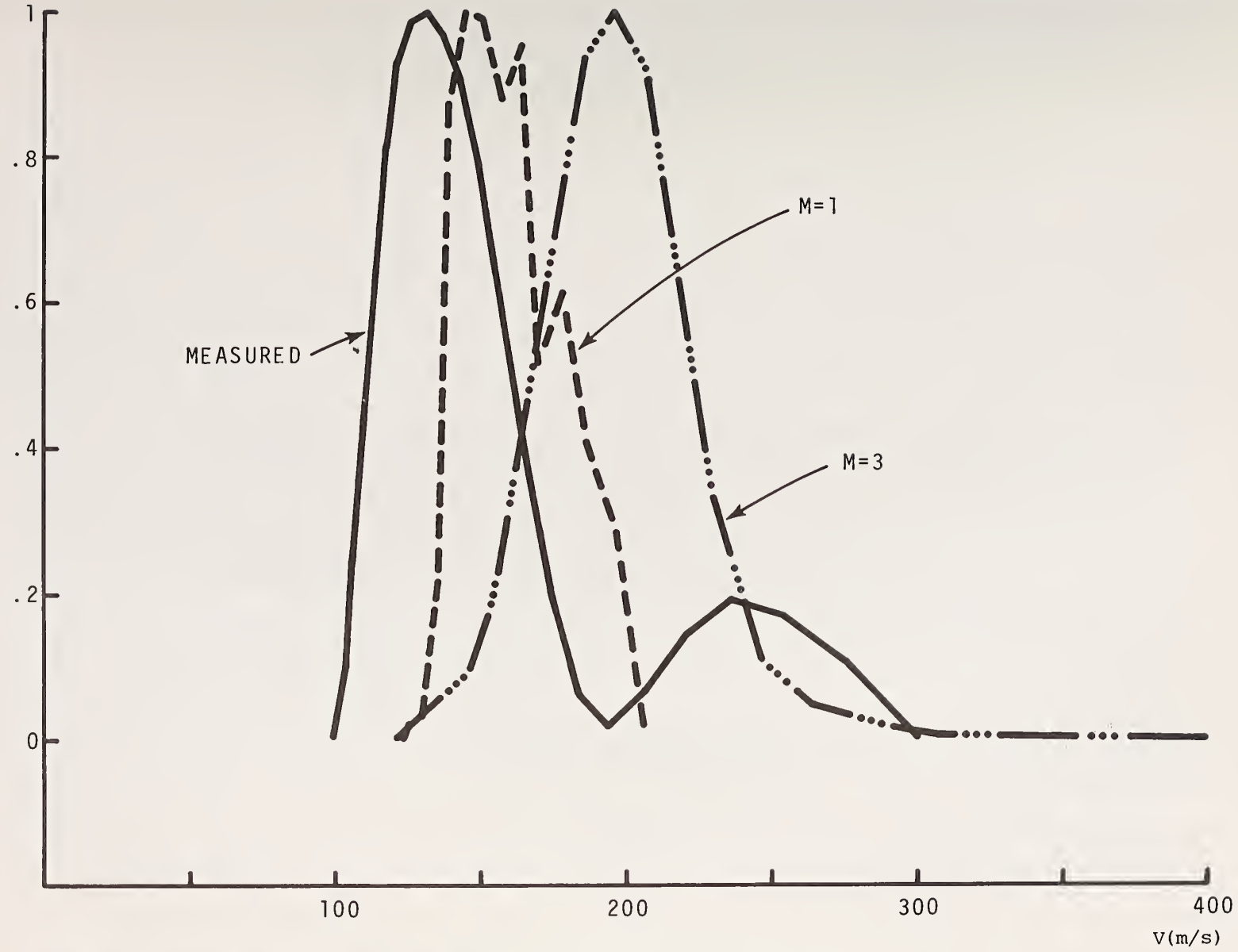

FIGURE 3: Measured and Simulated Velocity Distributions (normalized) for Tube B.

TABLE 1

Rf-Field Coefficients

Coefficient		C_2	C_3	C_4	C_6	C_7	C_{13}
Derivative		δ_z	δ_y	δ_{zz}	δ_{yy}	δ_x	δ_{xx}
rf-FIELD TYPE	1	0	-.387	.069	-.155	0	.124
	2	0	-.426	.076	-.170	0	.136
	3	-.003	-.404	.072	-.163	.006	.130

1. Principal h_2^j (ν) Field Expansion Coefficients by r-f Field Type. (See pp. 11, 17).

TABLE 2

K	S	M	(δ_z) σ_4	(δ_y) σ_5	(δ_{zz}) σ_6	(δ_{yy}) σ_8	(δ_x) σ_9	(δ_{xx}) σ_{16}	(δ_z) σ_{22}	(δ_y) σ_{23}	(δ_{zz}) σ_{24}	(δ_{yy}) σ_{26}	(δ_x) σ_{27}	(δ_{xx}) σ_{33}	b
1	1	2	-0.59	0	0.64	1.35	-0.63	1.02	1.86	0	-0.95	-1.45	-0.63	-1.02	15000
			-0.18	0	0.54	1.54	-2.10	1.01	2.50	0	-1.05	-1.42	-2.10	-1.01	25000
			0.49	0	0.38	1.88	-5.15	1.04	3.68	0	-1.23	-1.40	-5.15	-1.04	35000
		4	-0.32	0	0.80	1.07	-0.74	0.89	-0.99	0	-0.95	-1.13	-0.74	-0.89	15000
			-0.77	0	0.73	1.23	-2.63	0.88	-1.73	0	-0.95	-1.29	-2.63	-0.88	25000
			-1.15	0	0.58	1.54	-5.56	0.90	-2.79	0	-1.03	-1.53	-5.56	-0.90	35000
	2	2	-0.67	-1.09	0.65	1.34	-0.62	1.02	1.88	-0.96	-0.95	-1.47	-0.62	-1.02	15000
			-0.28	-1.29	0.55	1.52	-2.09	1.01	2.54	-0.77	-1.06	-1.44	-2.09	-1.01	25000
			0.38	-1.67	0.39	1.86	-5.16	1.04	3.78	-0.46	-1.26	-1.42	-5.16	-1.04	35000
		4	-0.28	-0.61	0.79	1.03	-0.74	0.89	-0.94	-0.69	-0.94	-1.13	-0.74	-0.89	15000
			-0.70	-0.77	0.71	1.17	-2.62	0.88	-1.66	-0.87	-0.94	-1.31	-2.62	-0.88	25000
			-1.03	-1.44	0.55	1.46	-5.49	0.91	-2.66	-1.17	-1.01	-1.58	5.49	-0.91	35000
2	1	1	6.59	0	1.19	2.96	-2.36	3.83	9.24	0	-1.90	-11.77	-2.36	-3.83	8000
			6.60	0	1.20	2.74	-9.22	3.58	9.76	0	-2.08	-12.00	-9.22	-3.58	14000
			6.63	0	1.21	2.22	-31.01	3.26	11.29	0	-2.61	-12.64	-31.01	-3.26	20000
		3	3.27	0	1.37	3.27	-2.00	4.54	6.82	0	-1.09	-5.92	-2.00	-4.54	8000
			2.95	0	1.44	3.19	-7.07	4.40	7.53	0	-1.24	-6.10	-7.07	-4.40	14000
			2.48	0	1.65	3.04	-18.86	4.22	8.91	0	-1.55	-6.50	-18.86	-4.22	20000
	2	1	5.99	-1.34	1.07	3.61	-2.36	3.84	9.34	-9.34	-1.94	-11.55	-2.36	-3.84	8000
			6.01	-1.20	1.08	3.39	-9.18	3.59	9.87	-10.28	-2.12	-11.78	-9.18	-3.59	14000
			6.18	-0.77	1.11	2.79	-30.67	3.29	11.41	-13.04	-2.66	-12.44	-30.67	-3.29	20000
		3	3.14	-1.24	1.37	3.13	-2.00	4.54	6.85	-4.40	-1.11	-6.00	-2.00	-4.54	8000
			2.77	-1.20	1.08	3.08	-7.08	4.39	7.57	-4.54	-1.26	-6.21	-7.08	-4.39	14000
			2.19	-1.12	1.11	2.98	-18.90	4.20	8.93	-4.83	-1.57	-6.62	-18.90	-4.20	20000

2. Principal PV-bias Multipliers $(\mu_n(b))$ for Each Cavity at Three Power Levels by Beam Tube Type (K = 1,2), y-Symmetry Condition (S = 1,2), and Detector Location (M). (See pp. 17).

TABLE 3

b^- x 10^{-4} (s^{-1})	1.0	1.5	2.0	2.5	3.0	3.5	4.0	4.5
V_D (cm/s)	29937	30367	31041	32048	33515	35506	37316	36104
V_P (cm/s)	29330	29742	30392	31375	32828	34826	36552	34830
h (mHz)	0.01	0.00	-0.02	-0.05	-0.09	-0.13	-0.14	-0.04
b^+ x 10^{-4} (s^{-1})	PV Power Shift Bias (mHz)							
1.5	-0.94							
2.0	-0.92	-0.91						
2.5	-0.89	-0.87	-0.85					
3.0	-0.84	-0.82	-0.80	-0.76				
3.5	-0.76	-0.74	-0.71	-0.67	-0.59			
4.0	-0.62	-0.60	-0.56	-0.49	-0.36	-0.07		
4.5	-0.30	-0.24	-0.13	0.11	0.81	649.	-1.89	

3. V_D, V_p, PV-bias $\mathcal{h}$, and Power Shift Biases for NBS-5 (S = 1, M = 2) for Cavity Fields (1 - ,1); b_{opt} = 24070 s^{-1}.

TABLE 4

b^- x 10^{-4} (s^{-1})	1.0	1.5	2.0	2.5	3.0	3.5	4.0	4.5
V_D (cm/s)	26270	26739	27502	28695	30484	32413	31148	26810
V_P (cm/s)	25767	26219	26955	28120	29886	31709	29909	25716
h (mHz)	0.00	0.00	0.00	0.00	-0.01	-0.03	-0.05	-0.03
b^+ x 10^{-4} (s^{-1})	PV Power Shift Bias (mHz)							
1.5	0.02							
2.0	0.00	-0.01						
2.5	-0.02	-0.03	-0.05					
3.0	-0.06	-0.07	-0.09	-0.12				
3.5	-0.13	-0.14	-0.17	-0.21	-0.31			
4.0	-0.28	-0.33	-0.42	-0.69	-46.6	0.32		
4.5	12.4	1.31	0.54	0.27	0.12	0.01	-0.10	

[4] - V_D, V_p, PV-bias $\hat{h}$, and Power Shift Biases for NBS-5 (S = 1, M = 4) for Cavity Fields (1 - 1); b_{opt} = 20840 s^{-1}.

TABLE 5

b^- x 10^{-4} (s^{-1})	1.0	1.5	2.0	2.5	3.0	3.5	4.0	4.5
V_D (cm/s)	30024	30444	31103	32091	33543	35548	37492	36522
V_P (cm/s)	29421	29823	30456	31416	32846	34849	36715	35248
h (mHz)	0.81	0.80	0.78	0.75	0.73	0.70	0.71	0.81
b^+ x 10^{-4} (s^{-1})	PV Power Shift Bias (mHz)							
1.5	-1.70							
2.0	-1.65	-1.63						
2.5	-1.60	-1.57	-1.53					
3.0	-1.52	-1.49	-1.45	-1.39				
3.5	-1.40	-1.37	-1.33	-1.26	-1.16			
4.0	-1.20	-1.17	-1.11	-1.02	-0.86	-0.50		
4.5	-0.78	-0.70	-0.56	-0.28	0.47	9.24	-3.29	

5. V_D, V_p, PV-bias $\mathcal{k}$, and Power Shift Biases for NBS-5 (S = 2, M = 2) for Cavity Fields (1 - 1); b_{opt} = 24130 s^{-1}.

TABLE 6

b^- x 10^{-4} (s^{-1})	1.0	1.5	2.0	2.5	3.0	3.5	4.0	4.5
V_D (cm/s)	26320	26802	27584	28804	30624	32566	31335	27005
V_P (cm/s)	25806	26286	27023	28216	30014	31825	30085	25875
h (mHz)	0.48	0.51	0.56	0.64	0.77	0.88	0.74	0.45
b^+ x 10^{-4} (s^{-1})	PV Power Shift Bias (mHz)							
1.5	1.32							
2.0	1.32	1.32						
2.5	1.31	1.31	1.30					
3.0	1.29	1.29	1.28	1.26				
3.5	1.25	1.24	1.22	1.20	1.12			
4.0	1.10	1.07	1.01	1.00	-11.8	1.67		
4.5	-11.3	3.54	2.10	1.71	1.53	1.42	1.34	

6. V_D, V_p, PV-bias n, and Power Shift Biases for NBS-5 (S = 2, M = 4) for Cavity Fields (1 - 1); b_{opt} = 20410 s^{-1}

TABLE 7

b^- x 10^{-4} (s^{-1})	0.5	0.8	1.1	1.4	1.7	2.0	2.3	2.6
V_D (cm/s)	15719	15787	15901	16085	16396	16968	17749	15394
V_P (cm/s)	15334	15382	15461	15586	15796	16188	16804	15502
h (mHz)	0.58	0.62	0.70	0.83	1.09	1.65	2.83	1.11
b^+ x 10^{-4} (s^{-1})	PV Power Shift Bias (mHz)							
0.8	13.3							
1.1	13.9	14.3						
1.4	14.8	15.2	15.8					
1.7	16.3	16.6	17.2	18.0				
2.0	18.5	18.9	19.4	20.2	21.4			
2.3	22.9	23.2	23.8	24.7	26.2	29.4		
2.6	48.4	62.6	156.	-52.5	-2.54	10.9	19.3	

7. V_D, V_p, PV-bias $\hbar$, and Power Shift Biases for Tube B (S = 1, M = 1) for Cavity Fields (1 - 1) b_{opt} = 12430 s^{-1}.

TABLE 8

$b^- \times 10^{-4}$ (s^{-1})	0.5	0.8	1.1	1.4	1.7	2.0	2.3	2.6
V_D (cm/s)	18491	18619	18816	19101	19499	20050	20764	21285
V_P (cm/s)	17946	18057	18230	18476	18816	19278	19856	20199
h (mHz)	0.49	0.48	0.46	0.44	0.40	0.35	0.28	0.25
$b^+ \times 10^{-4}$ (s^{-1})	PV Power Shift Bias (mHz)							
0.8	-2.15							
1.1	-2.18	-2.19						
1.4	-2.22	-2.23	-2.26					
1.7	-2.27	-2.29	-2.32	-2.36				
2.0	-2.34	-2.35	-2.38	-2.42	-2.47			
2.3	-2.40	-2.42	-2.45	-2.48	-2.53	-2.57		
2.6	-2.37	-2.38	-2.40	-2.42	-2.44	-2.42	-2.15	

8. V_D, V_p, PV-bias $\hbar$, and Power Shift Biases for NBS-5 (S = 1, M = 3) for Cavity Fields (3 - 2); b_{opt} = 14840 s^{-1}.

TABLE 9

b^- x 10^{-4} (s^{-1})	0.5	0.8	1.1	1.4	1.7	2.0	2.3	2.6
V_D (cm/s)	15757	15827	15943	16132	16449	17030	17807	15454
V_P (cm/s)	15369	15418	15500	15630	15848	16254	16874	15532
h (mHz)	5.28	5.37	5.51	5.74	6.12	6.80	7.53	4.37
b^+ x 10^{-4} (s^{-1})	Pv Power Shift Bias (mHz)							
0.8	21.4							
1.1	21.5	21.5						
1.4	21.6	21.6	21.7					
1.7	21.6	21.6	21.6	21.6				
2.0	21.1	21.1	21.0	20.9	20.5			
2.3	17/7	17.5	17.3	16.8	15.7	12.3		
2.6	-91.7	-140.	-549.	214.	81.8	48.0	32.2	

9. V_D, V_p, PV-bias h, and Power Shift Biases for NBS-5 (S = 2, M = 1) for Cavity Fields (1 - 1); b_{opt} = 12460 s^{-1}

TABLE 10

b^- x 10^{-4} (s^{-1})	0.5	0.8	1.1	1.4	1.7	2.0	2.3	2.6
V_D (cm/s)	18468	18594	18788	19067	19453	19980	20649	21083
V_P (cm/s)	17928	18039	18209	18450	18781	19220	19758	20016
h (mHz)	2.73	2.75	2.80	2.86	2.95	3.08	3.27	3.45
b^+ x 10^{-4} (s^{-1})	PV Power Shift Bias (mHz)							
0.8	1.55							
1.1	1.63	1.68						
1.4	1.74	1.79	1.88					
1.7	1.92	1.97	2.06	2.20				
2.0	2.19	2.25	2.35	2.51	2.75			
2.3	2.64	2.71	2.84	3.03	3.33	3.83		
2.6	3.50	3.62	3.83	4.16	4.73	5.90	10.4	

10. V_D,V_p, PV-bias h, and Power Shift Biases for NBS-5 (S = 2, M = 3) for Cavity Fields (1 - 3); b_{opt} = 14810 s^{-1}

NBS-114A (REV. 7-73)

U.S. DEPT. OF COMM. BIBLIOGRAPHIC DATA SHEET	1. PUBLICATION OR REPORT NO. NBS TN-660	2. Gov't Accession No.	3. Recipient's Accession No.

4. TITLE AND SUBTITLE

MOLECULAR BEAM TUBE FREQUECY BIASES DUE TO DISTRIBUTED CAVITY PHASE VARIATIONS.

5. Publication Date: January 1975

6. Performing Organization Code

7. AUTHOR(S): STEPHEN JARVIS, JR.

8. Performing Organ. Report No.

9. PERFORMING ORGANIZATION NAME AND ADDRESS

NATIONAL BUREAU OF STANDARDS, Boulder Labs.
DEPARTMENT OF COMMERCE
WASHINGTON, D.C. 20234

10. Project/Task/Work Unit No. 2770246

11. Contract/Grant No.

12. Sponsoring Organization Name and Complete Address *(Street, City, State, ZIP)*

13. Type of Report & Period Covered

14. Sponsoring Agency Code

15. SUPPLEMENTARY NOTES

16. ABSTRACT *(A 200-word or less factual summary of most significant information. If document includes a significant bibliography or literature survey, mention it here.)*

For atomic beam frequency standards, an analysis is described for estimating the frequency bias due to distributed cavity phase difference over finite beam widths, and for estimating the resulting inaccuracy in power shift and beam reversal experiments. Calculated atomic trajectories and simplified rf-field distributions are used, as well as certain assumptions about beam tube alignment. The results are applied to one of the present NBS primary time & frequency standards and a shorter tube geometry.

One conclusion is that beam reversal experiments are not necessarily much more accurate than power shift experiments and that the use of both methods (plus the use of pulse techniques) is desirable.

17. KEY WORDS *(six to twelve entries; alphabetical order; capitalize only the first letter of the first key word unless a proper name; separated by semicolons)*

Accuracy evaluation; Atomic beam frequency standards; Cavity phase shift

18. AVAILABILITY [X] Unlimited

[ ] For Official Distribution. Do Not Release to NTIS

[ ] Order From Sup. of Doc., U.S. Government Printing Office Washington, D.C. 20402, SD Cat. No. C13

[ ] Order From National Technical Information Service (NTIS) Springfield, Virginia 22151

19. SECURITY CLASS (THIS REPORT) UNCLASSIFIED

21. NO. OF PAGES 43

20. SECURITY CLASS (THIS PAGE) UNCLASSIFIED

22. Price $1.00

USCOMM-DC 29042-P74

NBS TECHNICAL PUBLICATIONS

PERIODICALS

JOURNAL OF RESEARCH reports National Bureau of Standards research and development in physics, mathematics, and chemistry. Comprehensive scientific papers give complete details of the work, including laboratory data, experimental procedures, and theoretical and mathematical analyses. Illustrated with photographs, drawings, and charts. Includes listings of other NBS papers as issued.

Published in two sections, available separately:

- **Physics and Chemistry (Section A)**

Papers of interest primarily to scientists working in these fields. This section covers a broad range of physical and chemical research, with major emphasis on standards of physical measurement, fundamental constants, and properties of matter. Issued six times a year. Annual subscription: Domestic, $17.00; Foreign, $21.25.

- **Mathematical Sciences (Section B)**

Studies and compilations designed mainly for the mathematician and theoretical physicist. Topics in mathematical statistics, theory of experiment design, numerical analysis, theoretical physics and chemistry, logical design and programming of computers and computer systems. Short numerical tables. Issued quarterly. Annual subscription: Domestic, $9.00; Foreign, $11.25.

DIMENSIONS/NBS (formerly Technical News Bulletin)—This monthly magazine is published to inform scientists, engineers, businessmen, industry, teachers, students, and consumers of the latest advances in science and technology, with primary emphasis on the work at NBS.

DIMENSIONS/NBS highlights and reviews such issues as energy research, fire protection, building technology, metric conversion, pollution abatement, health and safety, and consumer product performance. In addition, **DIMENSIONS/NBS** reports the results of Bureau programs in measurement standards and techniques, properties of matter and materials, engineering standards and services, instrumentation, and automatic data processing.

Annual subscription: Domestic, $9.45; Foreign, $11.75

NONPERIODICALS

Monographs—Major contributions to the technical literature on various subjects related to the Bureau's scientific and technical activities.

Handbooks—Recommended codes of engineering and industrial practice (including safety codes) developed in cooperation with interested industries, professional organizations, and regulatory bodies.

Special Publications—Include proceedings of high-level national and international conferences sponsored by NBS, precision measurement and calibration volumes, NBS annual reports, and other special publications appropriate to this grouping such as wall charts and bibliographies.

Applied Mathematics Series—Mathematical tables, manuals, and studies of special interest to physicists, engineers, chemists, biologists, mathematicians, computer programmers, and others engaged in scientific and technical work.

National Standard Reference Data Series—Provides quantitative data on the physical and chemical properties of materials, compiled from the world's literature and critically evaluated. Developed under a world-wide program coordinated by NBS. Program under authority of National Standard Data Act (Public Law 90-396).

Building Science Series—Disseminates technical information developed at the Bureau on building materials, components, systems, and whole structures. The series presents research results, test methods, and performance criteria related to the structural and environmental functions and the durability and safety characteristics of building elements and systems.

Technical Notes—Studies or reports which are complete in themselves but restrictive in their treatment of a subject. Analogous to monographs but not so comprehensive in scope or definitive in treatment of the subject area. Often serve as a vehicle for final reports of work performed at NBS under the sponsorship of other government agencies.

Voluntary Product Standards—Developed under procedures published by the Department of Commerce in Part 10, Title 15, of the Code of Federal Regulations. The purpose of the standards is to establish nationally recognized requirements for products, and to provide all concerned interests with a basis for common understanding of the characteristics of the products. The National Bureau of Standards administers the Voluntary Product Standards program as a supplement to the activities of the private sector standardizing organizations.

Federal Information Processing Standards Publications (FIPS PUBS)—Publications in this series collectively constitute the Federal Information Processing Standards Register. The purpose of the Register is to serve as the official source of information in the Federal Government regarding standards issued by NBS pursuant to the Federal Property and Administrative Services Act of 1949 as amended, Public Law 89-306 (79 Stat. 1127), and as implemented by Executive Order 11717 (38 FR 12315, dated May 11, 1973) and Part 6 of Title 15 CFR (Code of Federal Regulations). FIPS PUBS will include approved Federal information processing standards information of general interest, and a complete index of relevant standards publications.

Consumer Information Series—Practical information, based on NBS research and experience, covering areas of interest to the consumer. Easily understandable language and illustrations provide useful background knowledge for shopping in today's technological marketplace.

NBS Interagency Reports—A special series of interim or final reports on work performed by NBS for outside sponsors (both government and non-government). In general, initial distribution is handled by the sponsor; public distribution is by the National Technical Information Service (Springfield, Va. 22151) in paper copy or microfiche form.

Order NBS publications (except Bibliographic Subscription Services) from: Superintendent of Documents, Government Printing Office, Washington, D.C. 20402.

BIBLIOGRAPHIC SUBSCRIPTION SERVICES

The following current-awareness and literature-survey bibliographies are issued periodically by the Bureau:

Cryogenic Data Center Current Awareness Service (Publications and Reports of Interest in Cryogenics). A literature survey issued weekly. Annual subscription: Domestic, $20.00; foreign, $25.00.

Liquefied Natural Gas. A literature survey issued quarterly. Annual subscription: $20.00.

Superconducting Devices and Materials. A literature survey issued quarterly. Annual subscription: $20.00. Send subscription orders and remittances for the preceding bibliographic services to the U.S. Department of Commerce, National Technical Information Service, Springfield, Va. 22151.

Electromagnetic Metrology Current Awareness Service (Abstracts of Selected Articles on Measurement Techniques and Standards of Electromagnetic Quantities from D-C to Millimeter-Wave Frequencies). Issued monthly. Annual subscription: $100.00 (Special rates for multi-subscriptions). Send subscription order and remittance to the Electromagnetic Metrology Information Center, Electromagnetics Division, National Bureau of Standards, Boulder, Colo. 80302.

U.S. DEPARTMENT OF COMMERCE
National Bureau of Standards
Washington, D.C. 20234

OFFICIAL BUSINESS

Penalty for Private Use, $300

POSTAGE AND FEES PAID
U.S. DEPARTMENT OF COMMERCE
COM-215

U.S.MAIL

AMERICAN REVOLUTION BICENTENNIAL 1776-1976

☆GPO 1974 — 677-237/1233 REGION NO. 8